J|A|C|S
ARTICLES
Published on Web 10/31/2007

DNA Sensing by Field-Effect Transistors Based on Networks of Carbon Nanotubes

Ee Ling Gui,[†] Lain-Jong Li,*[,†] Keke Zhang,[†] Yangping Xu,[†] Xiaochen Dong,[†] Xinning Ho,[‡] Pooi See Lee,[†] Johnson Kasim,[§] Z. X. Shen,[§] John. A. Rogers,[‡] and S.G. Mhaisalkar[†]

Contribution from the School of Materials Science and Engineering, Nanyang Technological University 50, Nanyang Avenue, Singapore, 639798, Department of Materials Science and Engineering, and Department of Chemistry, University of Illinois at Urbana-Champaign, Illinois 61801, and School of Physical and Mathematical Science, Nanyang Technological University, 50 Nanyang Avenue, Singapore 639798

Received July 11, 2007; E-mail: ljli@ntu.edu.sg

Abstract: We report on the sensing mechanism of electrical detection of deoxyribonucleic acid (DNA) hybridization for Au- and Cr-contacted field effect transistors based on single-walled carbon nanotube (SWCNT) networks. Barrier height extraction via low-temperature electrical measurement provides direct evidence for the notion that the energy level alignment between electrode and SWCNTs can be affected by DNA immobilization and hybridization. The study of location-selective capping using photoresist provides comprehensive evidence that the sensing of DNA is dominated by the change in metal−SWCNT junctions rather than the channel conductance.

Introduction

Single-walled carbon nanotubes (SWCNTs) have attracted much attention in sensor applications because they are highly sensitive to molecular adsorption on the tube wall[1] or within the tubes.[2] Label-free electrical detection of deoxyribonucleic acid (DNA) and biomolecules using networked carbon nanotube field-effect transistors (FETs) have recently been achieved.[3−4] A reduction−oxidation sensitive intercalator has also been demonstrated to largely enhance the sensitivity of these devices.[4] Recently, contrasting mechanisms for the electrical detection of DNA hybridization, channel dependent[3,5] as opposed to contact modulation,[6] have been reported. In the former, the electrical conductance change is suggested to be resulting from the electron doping by DNA hybridization directly on the carbon nanotubes,[3,5] whereas, in the latter, the change in the metal−SWCNT barrier energy through the modulation of the electrode work function[6] was related to the detection of DNA hybridization. Furthermore, the channel dependence observations were primarily based on fluorescence studies[3] which confirmed the presence of hybridized DNA in contact with the SWCNT channel, whereas the channel modulation study was based on the observation that the complementary DNA hybridized with the thiolated capture probe DNA only on the Au electrodes but not on SWCNTs.[6] Note that the capture probe DNA serves as a platform for binding with complementary DNA in the process known as hybridization. Capping or junction blocking studies and use of capture probe DNA with binding affinity to both Au electrodes and SWCNTs were not used by either of these studies, and direct evidence of the dominant role of junction versus the channel in electrical sensing was not imminent. Thus for SWCNT network devices, a complete understanding of the interaction among the capture probe DNA, hybridized DNA, and SWCNT−electrode contacts is key in elucidating the sensing mechanism and warrants further studies.

In this report, the observation from fluorescence microscopy suggests that the DNA binding to SWCNTs does occur in the channel area (between source and drain contacts), which accounts for part of the drain current (I_d) change. We have also examined the electrical detection of DNA hybridization for SWCNT networked FETs (SNFETs) with two different contacts (Au−SWCNT and Cr−SWCNT). The drain current for Au-contacted devices was decreased upon DNA hybridization, consistent with previous reports.[3−4] By contrast, I_d in Cr-contacted devices was increased, suggesting that the change in the electrode−SWCNT interface should contribute significantly to electrical signals, which is corroborated with the observed change in the activation energy barrier of the thermal emission current through the SWCNT−electrode junctions.

[†] School of Materials Science and Engineering, Nanyang Technological University.
[‡] University of Illinois at Urbana-Champaign.
[§] School of Physical and Mathematical Science, Nanyang Technological University.

(1) Kong, J.; Franklin, N. R.; Zhou, C.; Chapline, M. G.; Peng, S.; Cho, K.; Dai, H. *Science* **2000**, *287*, 622−625.
(2) Li, L. J.; Khlobystov, A. N.; Wiltshire, J. G.; Briggs, G. A. D.; Nicholas, R. J. *Nat. Mater.* **2005**, *4*, 481−485.
(3) Star, A.; Tu, E.; Niemann, J.; Gabriel, J. C. P.; Joiner, C. S.; Valcke, C. *Proc. Natl. Acad. Sci. U.S.A.* **2006**, *103*, 921−926.
(4) Gui, E. L.; Li, L. J.; Lee, P. S.; Lohani, A.; Mhaisalkar, S. G.; Cao, Q.; Kang, K.; Rogers, J. A.; Tansil, N. C.; Gao, Z. *Appl. Phys. Lett.* **2006**, *89*, 232104/1−232104/3.
(5) Star, A.; Gabriel, J. C. P.; Bradley, K.; Gruner, G. *Nano Lett.* **2003**, *3*, 459−463.
(6) Tang, X.; Bansaruntip, S.; Nakayama, N.; Yenilmez, E.; Chang, Y. I.; Wang, Q. *Nano Lett.* **2006**, *6*, 1632−1636.

10.1021/ja075176g CCC: $37.00

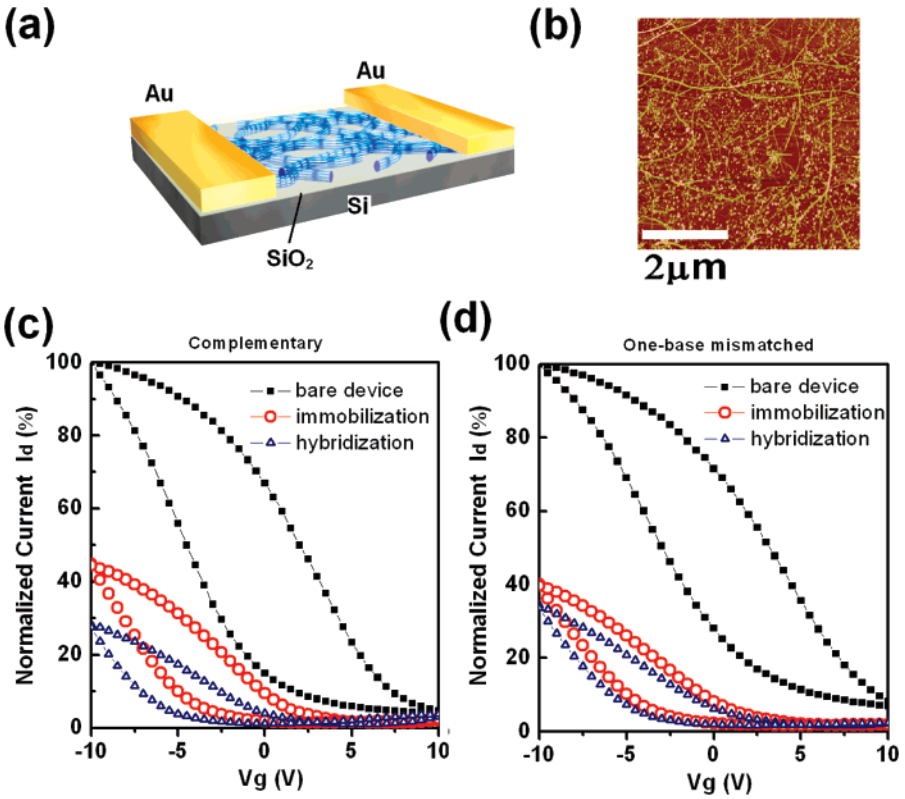

Figure 1. (a) Schematic illustration of the networked devices, (b) a typical atomic force microscope image on the SWCNT channel, (c,d) typical gate voltage dependence of the normalized drain current I_d for (c) a CNFET bare device, immobilized with probe−DNA and hybridized with complementary target analyte and (d) a CNFET bare device, immobilized with probe−DNA and hybridized with single-base mismatched target analyte (source−drain bias was kept at −0.5 V).

Experimental Section

Random networks of SWCNTs with diameters between 1 and 3 nm and lengths between 5 and 10 μm were first grown onto SiO_2 (100 nm)/Si wafers using chemical vapor deposition techniques. SWCNT network transistors (SNFETs) were fabricated in a top contact device geometry (illustrated in Figure 1a), where 30 nm of Au electrodes (as Au−SWCNT contact) or 3 nm Cr/30 nm Au (as Cr−SWCNT contact) were patterned on top of it using standard lithography techniques.[7−9] The channel lengths of the devices investigated were 2, 10, 25, and 50 μm. For the drop-cast procedure, 50 μL of SWCNT suspension was added on the devices, followed by drying and rinsing of deionized water, where the SWCNT suspensions were prepared as follows: 10 mg of HiPCO SWNTs (from Carbon Nanotech. Inc., USA) were dispersed in 100 mL of D_2O solution with 1 wt % sodium dodecyl sulfate (SDS). The dispersion was then treated by probe sonication (Sonics & Materials Inc., Model: VCX 130) at a power level of 250 W for 30 min, followed by ultracentrifugation at 140 000 g-force for 4 h. For immobilization, SNFETs were immersed in 1 μM synthetic oligonucleotide in Tris-ethylenediaminetetraacetic acid (Tris-EDTA) buffer solution (10 mM tris-HCl/1.0 mM EDTA/0.10M NaCl) for a period of 16−24 h. A standard rinsing with Tris-EDTA buffer was performed to remove the weakly bound DNA molecules, and SNFETs were blown dry before electrical characterization. For hybridization experiments, 10 μL of 500 nM complementary target analyte (unlabeled or fluorescent labeled) were pipetted onto the immobilized SNFETs and allowed to react for 1 h, followed by washing and drying. The sequences of the synthetic probe, its one-base mismatched, and complementary oligonucleotides were 5′-AGG-TCG-CCG-CCC-$(CH_2)_3NH_2$, 5′-GTG-CGG-CGA-CCT, and 5′-GGG-CGG-CGA-CCT, respectively. A confocal Raman microscope (WITec CRM200) was used in this study for PL and Raman imaging. A double-frequency Nd:YAG excitation laser with a wavelength of 532 nm was coupled into the system with single mode fiber. The power of the laser on the sample can be adjusted with a linear continuous variable filter. The PL and Raman signals were collected via backscattering configuration (Olympus 100X objective lens, NA 0.95) to a TE-cooled CCD. The diameter of the laser spot was around 300 nm, and the sample was scanned using a piezoelectric stage. All electrical measurements were carried on in a N_2 glovebox or in a vacuum using a Kiethley semiconductor parameter analyzer Model 4200-SCS.

Results and Discussion

Figure 1a and b, respectively, show the schematic illustration of the networked devices and a typical atomic force microscope image demonstrating the density of SWCNTs and catalyst particles on them. Figure 1c shows the typical gate voltage dependence of the normalized I_d for an SNFET device, immobilized with a capture probe DNA and hybridized with complementary target analytes, and Figure 1d demonstrates the parallel results for the device hybridized with single-base mismatched analytes. The electrical differentiation of the complemenary and mismatched DNA species is achieved by comparing the difference in percentage reduction of I_d that occurred due to hybridization.[3−4] The large reduction in I_d after immobilization has been attributed to attachment of DNA molecules on the sidewalls of SWCNTs resulting in electron doping to the SWCNT semiconductor channels.[5] We believe it only accounts for part of the I_d reduction, and the modulation

(7) Hur, S. H.; Kocabas, C.; Gaur, A.; Shim, M.; Park, O. O.; Rogers, J. A. *J. Appl. Phys.* **2005**, *98*, 114302/1−114302/6.
(8) Hur, S. H.; Khang, D. Y.; Kocabas, C.; Rogers, J. A. *Appl. Phys. Lett.* **2004**, *85*, 5730−5732.
(9) Zhou, Y.; Gaur, A.; Hur, S. H.; Kocabas, C.; Meitl, M.; Shim, M.; Rogers, J. A. *Nano Lett.* **2004**, *4*, 2031−2035.

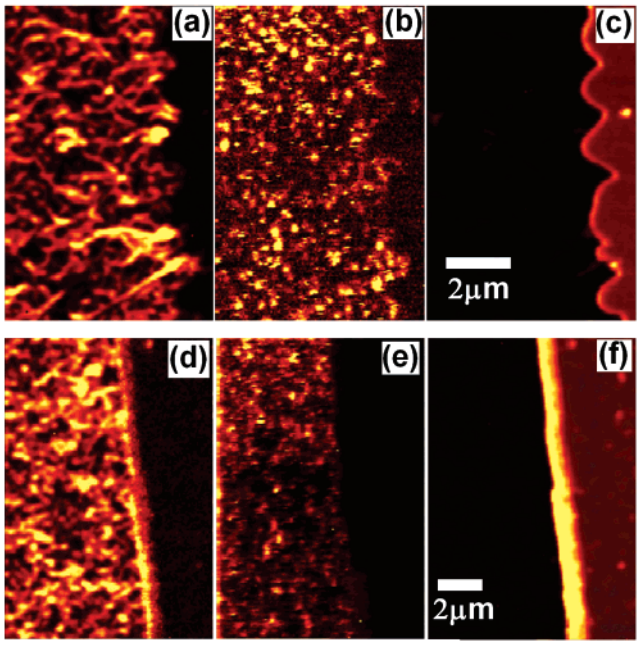

Figure 2. Comparison of the fluorescence signal from Cy3 tagged complementary DNA and mismatched DNA. (a) Raman map of G mode intensity, (b) fluorescence map, and (c) Device channel−electrode profile for an SNFET immobilized with a DNA probe and hybridized with Cy-3 labeled complementary target DNA. (d) Raman map of G mode intensity, (e) fluorescence map, and (f) device channel−electrode profile for an SNFET immobilized with a DNA probe and hybridized with Cy-3 labeled mismatched DNA.

of the electrode−SWCNT contact also largely contributes to the I_d reduction, which will be further discussed later.

It is well accepted that a single strand DNA can strongly interact with SWCNTs,[10−11] and Tang et al. observed that DNA binds to SWCNT sidewalls irreversibly.[6] Here we examine the interaction between DNA and the SWCNTs in the device channel area using confocal Raman and fluorescence microscopy. Figure 2a shows the Raman mapping of integrated peak area of G modes from the carbon nanotubes on a selected area of the device. Nanotubes can be clearly identified in this map although there is some thickening due to the limit in optical resolution (∼300 nm in our study). Figure 2b shows a fluorescent map of the same device area with capture probe DNA and hybridization with Cy3 dye-labeled complementary DNA, followed by thorough washing to remove the excess and weakly bound species. Figure 2c shows the metal profile defined in the same selected area. From Figure 2a and 2b, the fluorescence was mostly observed from the area covered with carbon nanotubes, suggesting a selective binding between complementary target DNA and capture probe DNA. Parallel studies using Cy3-tagged mismatched DNA (Figures 2d−f) indicate visibly weaker fluorescence, thus confirming minimal nonspecific binding between mismatched DNA in the channel area. It is noted that very weak fluorescence was observed from the electrode area due to nonradiative energy transfer from Cy3 to metal surfaces.[12] The selective DNA binding or nonspecific binding between DNA and SWCNTs in the channel area are expected to reduce the I_d upon hybridization through electronic doping or increasing scattering sites.[5] However, modulation of the electrode−SWCNT contact is also a possible explanation, and therefore we performed a series of studies to address this issue.

Figure 3a and b show, respectively, the typical transfer curves for SNFETs with a Au−SWCNT and a Cr−SWCNT contact (channel length = 50 μm) before immobilization, after immobilization, and upon hybridization with its complementary DNA. The immobilization process significantly reduced the on-state I_d for both Au-contacted (∼55.2% reduction at gate voltage (V_g) = −10 V) and Cr-contacted devices (∼ 99.7% reduction at V_g = −10 V). The subsequent hybridization further reduces the I_d for the Au-contacted device, whereas the I_d for the Cr-contacted device increases. These observations suggest that the electrical sensing is strongly related to the metal−SWCNT contact. Table 1 compiles the effect of DNA binding and hybridization on threshold voltage (V_{th}) and apparent hole mobility extracted from the transfer characteristics. A decrease in V_{th} across all devices was observed, with a consistent V_{th} shift from ∼8 to ∼24 V for bare devices to ∼2 to ∼7 V for devices after immobilization. This effect observed for both Au- and Cr-contacted devices indicates a possible electronic doping of SNFETs from the capture probe DNA, an observation also previously reported in the literature.[3] The hybridization further decreases the V_{th} of both types of devices, which suggests a further reduction in the hole concentration and thus a decrease in conductance for both types of SWCNT devices. However, contrary to this view of decreasing conductance, the Cr−SWCNT devices register an increase in I_d in their transition from immobilization to hybridization stages (Figure 3b). This observation suggests that the electronic doping or increase of scattering centers may not be the only major contributing factor for DNA sensing. Interestingly the evolution of the apparent mobility for Cr−SWCNT contacted devices agrees well with the change in I_d. The change in apparent mobility implies a change in either intertube contact resistance or electrode−SWCNT contact resistance (or junction barrier height). We would expect to see a consistent change in apparent mobility (mobility decrease in both Au and Cr contacts) if the DNA hybridization effects an increase in intertube contact resistance.[7,13] The fact that upon hybridization the apparent mobility and I_d in Cr-contacted devices increase but decrease in Au-contacted devices strongly corroborates the theory that the sensing of DNA hybridization is mainly contributed from the contact resistance change of metal−SWCNT junctions. To confirm the contribution from the junction we deposited another layer of networked SWCNTs onto the Cr-contacted device by drop-casting. Upon the addition of drop-casted SWCNTs, the Cr-SNFETs change its characteristics and now resemble Au-SNFETs, because the additional nanotubes cover the whole surface of Au and existing SWCNT networks and provide a continuous Au-drop-casted-SWCNT−SWCNT network contact as illustrated in the inset of Figure 3c. The transfer characteristics for these "dual contact" devices (Figure 3c) illustrate that upon hybridization the I_d decreases rather than increases, demonstrating a Au-contacted characteristic similar to that for Figure 3a and providing further credence to the notion that the metal−

(10) Zheng, M.; Jagota, A.; Semke, E. D.; Diner, B. A.; McLean, R. S.; Lustig, S. R.; Richardson, R. E.; Tassi, N. G. *Nat. Mater.* **2003**, *2*, 338−342.
(11) Lu, G.; Maragakis, P.; Kaxiras. E. *Nano Lett.* **2005**, *5*, 897−900.
(12) Rant, U.; Arinaga, K.; Fujiwara, T.; Fujita, S.; Tornow, M.; Yokoyama, N.; Abstreiter, G. *Biophys. J.* **2003**, *85*, 3858−3864.
(13) Hecht, D. S.; Ramirez, R. J. A.; Briman, M.; Artukovic, E.; Chichak, K. S.; Stoddart, J. F.; Gruner, G. *Nano Lett.* **2006**, *6*, 2031−2036.

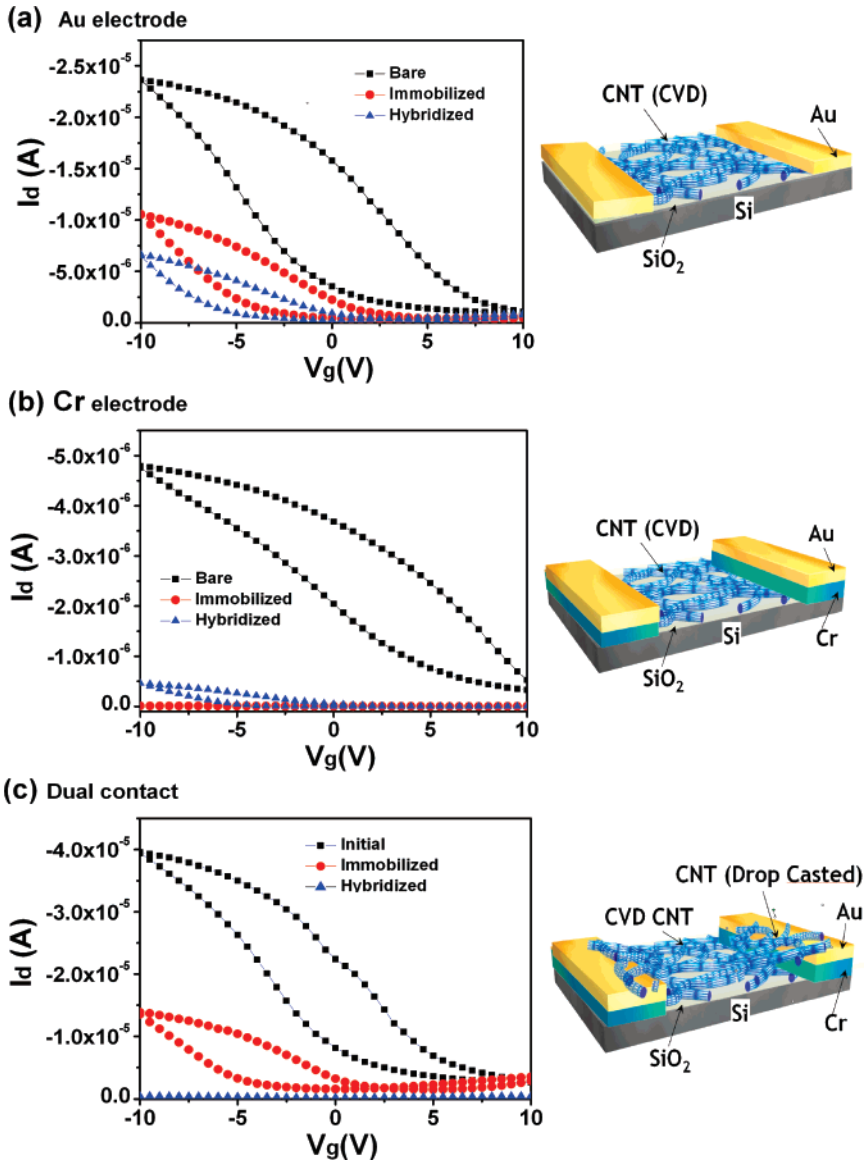

Figure 3. Typical transfer curves for SNFETs with (a) SWCNT−Au, (b) SWCNT−Cr, and (c) dual contact (channel length = 50 μm) before immobilization, after immobilization, and upon hybridization with its complementary DNA, where the drain voltage was fixed at −0.5 V. The dual contact device is produced by drop casting extra SWCNTs on an SWCNT−Cr contacted device.

Table 1. Effect of DNA Binding and Hybridization on Threshold Voltage and Percentage Change in Apparent Hole Mobility Extracted from the Transfer Characteristics[a]

channel length (μm)	change in apparent hole mobility (%)		threshold voltage (v)		
	on immobilization	on hybridization	bare	immobilized	hybridized
		Au−SWCNT Contacted			
2	−49.8 (+7.1)	−33.4 (±3.5)	10.1 (±1.3)	6.8 (±0.6)	3.6 (±0.5)
10	−51.2 (±3.7)	−22.0 (±1.9)	8.8 (±0.9)	4.2 (±0.4)	3.9 (±0.6)
50	−57.6 (±4.4)	−30.5 (±2.3)	7.8 (±0.3)	2.7 (±0.1)	2.4 (±0.3)
		Cr−SWCNT Contacted			
2	−76.3 (±1.6)	+41.1 (±1.0)	23.8 (±1.0)	8.3 (±2.4)	6.2 (±0.8)
10	−72.0 (±4.1)	+23.1 (±3.5)	21.4 (±2.1)	10.3 (±3.2)	7.9 (±3.9)
50	−78.6 (±2.5)	+21.3 (±2.1)	18.0 (±0.9)	3.8 (±0.2)	3.5 (±0.3)

[a] Each statistical number was based on three to four devices. The percentage change in apparent hole mobility on immobilization or on hybridization was all relative to the mobility of its bare device.

SWCNT contact should make a major contribution to the electrical detection of DNA hybridization.

We have also performed the area-selective photoresist blocking to reveal the effects of junction and channel on I_d. The Au-contacted devices were covered with a positive photoresist (EPG510), and the patterns were formed by lithography using a confocal microscope (with a 488 nm laser as light source for exposure). The width of the exposed area was kept at ~30 μm for each SNFET in this study. The evolution of transfer characteristics (before immobilization, after immobilization and

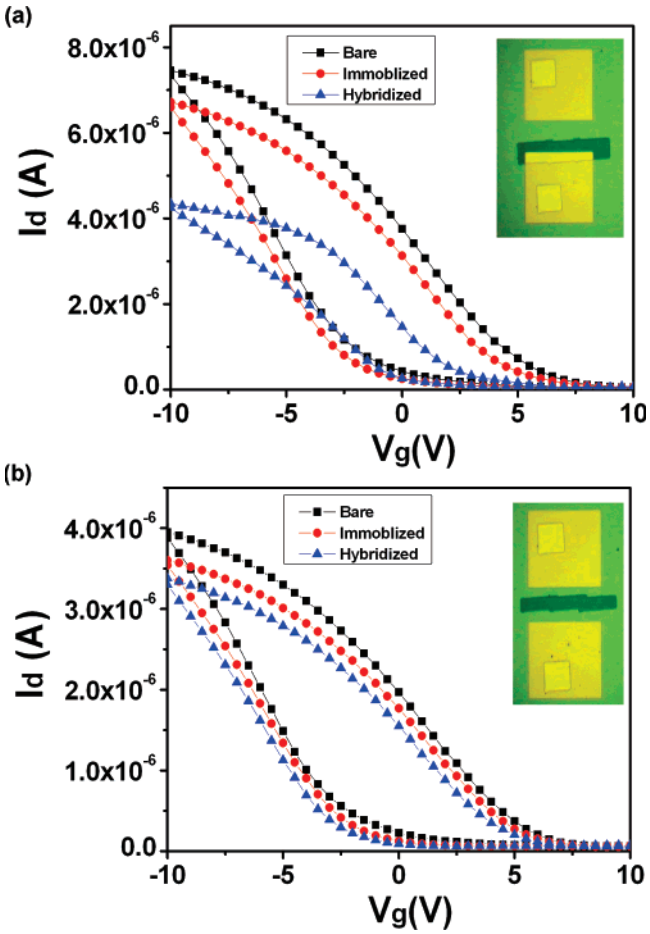

Figure 4. Transfer curves for photoresist capped Au-contacted SNFETs with (a) one junction exposed, (b) a channel exposed before immobilization, after immobilization, and upon hybridization with its complementary DNA, where the drain voltage was fixed at −0.5 V. The inset for each graph shows the photoresist pattern as imaged in an optical microscope.

hybridization with its complementary DNA) for the capped SNFETs with the junction or channel exposed are displayed in Figure 4a and b, respectively. It is observed that the percentage I_d decreases upon hybridization for the junction-exposed SNFET (∼31.8%), and it was only ∼5.6% for the channel-exposed SNFET, which further corroborates the theory that the junction plays a dominant role in sensing. The 5.6% drop in channel exposed SNFET is likely due to the electronic doping or increase of scattering centers (from nonspecific binding) as discussed before. The noncomplementary DNA has also been tested using junction-exposed Au-contacted SNFETs. The interaction between the immobilized SNFET with a noncomplementary DNA does not induce a significant change in I_d, which indicates that for the junction-exposed device the nonspecific binding is not pronounced in this case.

Now we consider the mechanism of molecular detection. To verify whether the DNA molecules affect the junction barrier energy, activation energy extraction was performed for devices before and after DNA immobilization and hybridization using the Arrhenius equation $I_d \approx \exp[-E_a/kT]$,[14−15] where E_a is the activation energy, k is the Boltzmann constant, and T is the temperature. Following methodologies described in the literature,[14] we kept the device at 10^{-7} Torr for at least 12 h and observed the n-channel formation due to the de-doping. For the interpretation of sensing results, we then extracted the estimated activation barrier energy for thermionic hole current in the temperature range from 160 to 230 K in a vacuum (10^{-7} Torr). The Arrhenius plot, with linearly fitted I_d−$1/T$ graphs at V_d = 0.01 V and V_g varying from −5 to +7 V is displayed in Figure 5a. The activation barrier energy (for holes) for Au−SWCNT contacted SNFET estimated at 69 meV in the bare device increases to 78 meV after immobilization and further increases to 85 meV after hybridization, as shown in Figure 5b. In the

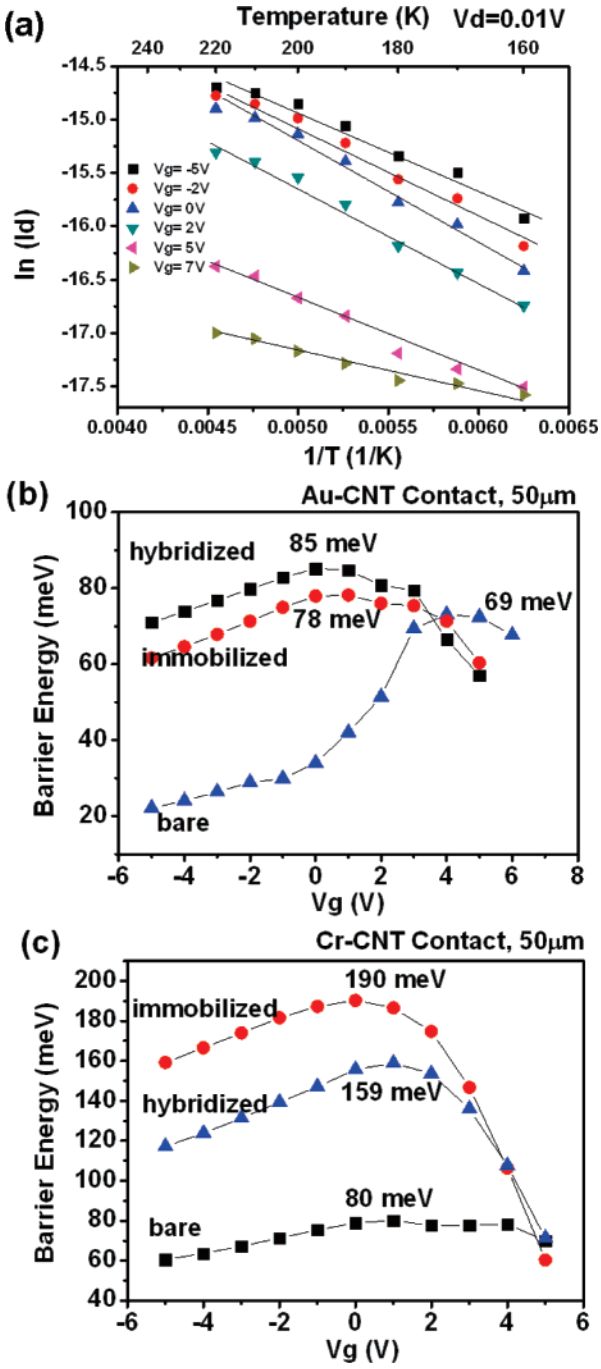

Figure 5. (a) Arrhenius plot (ln I_d vs $1/T$) of the Au−SWCNT contacted SNFET after immobilization; V_d = −0.02 V. (b,c) Extracted activation energy barriers vs applied gate voltage for (b) Au−SWCNT contacted and (c) Cr−SWCNT contacted SNFETs before and after immobilization and after hybridization (device channel length in both cases is 50 μm).

(14) Chen, Y. F.; Fuhrer, M. S. *Nano Lett.* **2006**, *6*, 2158−2162.
(15) Fukao, T.; Nakamura, S.; Kataura, H.; Shiraishi, M. *Jpn. J. Appl. Phys.* **2006**, *45*, 6524−6527.

Table 2. Channel Length Effect on Electrical Sensing of DNA[a]

channel length (um)	(%) change in I_d after DNA immobilization	(%) change in I_d after complementary DNA hybridization
	Au−SWCNT Devices	
2	−59.8	−33.3
5	−64.4	−11.6
10	−52.2	−26.1
50	−55.1	−16.9
	Cr−SWCNT Devices	
2	−79.6	+21.3
5	−86.7	+20.4
10	−71.0	+16.3
25	−82.9	+11.9
50	−82.8	+9.9

[a] Tabulated values of the percentage change in on-state I_d for Au- and Cr-contacted devices (at $V_g = -10$ V) and the percentage change after hybridization with complementary DNA. All values are relative to their bare devices.

case of Cr-contacted SNFET (shown in Figure 5c), the corresponding activation energies were 80, 190, and 159 meV for bare, immobilized, and hybridized devices, respectively. Note that the apparent decrease at a positive gate voltage (off-state of the transistor) could be due to a parallel metallic conductance channel existing in the device, for which conductance is probably temperature independent and contributing more at a positive gate voltage and thus giving a lower *effective* barrier height. The change in barrier energy for both Au- and Cr-contacted SNFETs corresponds *qualitatively* to the change in apparent mobilities as shown in Table 1; i.e. for the same device when the extracted barrier energy is higher a lower apparent mobility (or lower drain current) is observed, substantiating the conclusion that sensing is dominated by the junction. We have also studied the device channel length effect on the percentage change of I_d. Table 2 shows that for both Au−SWCNT and Cr−SWCNT contacted SNFETs the I_d change upon complementary DNA hybridization is larger in the short channel devices, corroborating again to sensing being dominated by junction modulation where we expect to see a larger fractional contribution of junction to I_d in a short channel device assuming that the total resistance of the device is simply an addition of junction and channel resistance. The data also suggest that increased device sensitivity is expected with shorter channel length devices and that scaling of transistors is indeed a key factor that needs to be considered in sensor design, an observation previously reported in organic thin film transistor based sensors.[16]

Several reports have suggested that the short-range dipole (or electrostatic) interaction near the actual electrode−SWCNT junction may interact with the junction and hence affect the energy level alignment.[17−18] The density of phosphate groups present within the DNA was believed to be responsible for the resulting surface charge on substrates, where the surface charges increased upon hybridization.[19] Another possible explanation was suggested by Steel et al.[20] that short single-stranded DNA were in a random coiled conformation while double-stranded DNA were rodlike in conformation and hence the change in DNA conformation results in the phosphate charge density change. It is likely that the change in charge density near the junction, from either the direct increase via hybridization or the change induced from the DNA conformation change, results in the direct modification of band alignment in the Au−SWCNT and Cr−SWCNT contacts. The different sensing behavior of Au- and Cr-contacted devices could be due to the different modifications of the band alignment near the junction areas.

Conclusions

In summary, different electrical characteristics upon DNA immobilization and hybridization were observed in Au- and Cr-contacted single walled carbon nanotube field effect transistors. Barrier height data provide direct evidence correlating electrode−SWCNT energy level alignment and DNA immobilization and hybridization, thus suggesting that the DNA sensing mechanism is through the charge density modification near the electrode−SWCNT junctions. The photoresist capping study demonstrated that the contribution of electrode−SWCNT junctions (~32% change in I_d) to DNA sensing was up to six times more pronounced than that of the SWCNT channel (~6% change in I_d). The detailed electrostatic interactions between DNA and electrode or between DNA and SWCNT require further detailed experimental and simulation studies. We believe that the results summarized here will stimulate better and alternate sensor designs that will exploit the pronounced interaction between analytes and the electrode−SWCNT junctions.

Acknowledgment. This research was supported by Nanyang Technological University, Singapore.

JA075176G

(16) Wang, L.; Fine, D.; Sharma, D.; Luisa, T.; Dodabalapur, A. *Anal. Bioanal. Chem.* **2006**, *384*, 310−321.
(17) Lang, N. D.; Avouris, P. *Nano Lett.* **2002**, *2*, 1047−1050.
(18) Cui, X.; Freitag, M.; Martel, R.; Brus, L.; Avouris, P. *Nano Lett.* **2003**, *6*, 783−787.
(19) Hansen, D. C.; Hansen, K. M.; Ferrell, T. L.; Thundat, T. *Langmuir* **2003**, *19*, 7514−7520.
(20) Steel. A. B.; Levicky, R. L.; Herne, T. M.; Tarlov, M. J. *Biophys. J.* **2000**, *79*, 975−981.